Information Masking Theory for Data Protection in Future Cloud-Based Energy Management

Shujun Xin, *Student Member, IEEE*, Qinglai Guo, *Senior Member, IEEE*, Jianhui Wang, *Senior Member, IEEE*, Chen Chen, *Member, IEEE*, Hongbin Sun, *Senior Member, IEEE*, and Boming Zhang, *Fellow, IEEE*

***Abstract*—Implementation of advanced information and communication technologies upgrades energy management systems (EMSs) by allowing more participants and improving the control ability, in which cloud-based service plays an essential role. However, its information exchange also raises concern about information safety and privacy. To overcome this challenge, we propose the mechanism of information masking (IM), which helps to hide the original information by transforming it to another form. In the main body, we first review the basic theory of IM. Then, we introduce three typical scenarios for cloud-based EMSs [i.e., home/building EMS (for end users), aggregated load/generation management (for aggregated loads), and coordinated dispatch (for multi-regional power systems)], then analyze and compare their IM requirements. After discussing the IM design rules for two general requirements, we discuss IM algorithms for the three scenarios and study three typical cases to verify the feasibility and effectiveness of the IM approaches. The results show that the proposed IM approaches successfully hide all the targeted information while leading to only minor increases in computation cost and matrix sparsity.**

***Index Terms*—Information security, data protection, network transformation, cloud computing, energy management system.**

I. Introduction

BECAUSE of the extensive implementation of advanced information and communication technologies (ICTs), highly efficient data transmission and exchange have gradually become indispensable for power systems and have exponentially upgraded the control ability and range of energy management systems (EMSs) [1], [2]. To dispatch more resources and serve diversified participants, such as home users, industrial parks and load aggregators, power system operators and researchers have tried to introduce state-of-the-art cloud computing technologies in future EMS design because of its near-infinite capacity for customers.

Currently, power system researchers and engineers have explored numerous cloud-based EMS applications for different levels of participants, including

- ➢ end users, such as homes and buildings [3], [4],
- ➢ agents, such as aggregated loads and generations [3], [4], and
- ➢ interconnected power systems.

The above-mentioned three levels of participants might require for different energy management services with different scales, but one thing they have in common is that their decision processes are no longer performed locally and require sufficient information transmission and exchange between the local and the cloud side. However, this unavoidable information exchange raises concern about information protection. Numerous studies investigating EMS applications have addressed information security as a key challenge [3], [5], [8]–[12]. According to previous studies, information disclosure may lead to personal dissatisfaction or inconvenience as well as serious consequences, such as data attacks, whose key precondition is perfect information about the power grid [13]–[16]. Therefore, a robust data protection mechanism is necessary for stable and secure operation of future cloud-based EMSs.

Most privacy-related research has focused on authentication and authorization to prevent malicious access to unauthorized data [8]. Recently, some researchers have explored another approach, namely, information masking (IM) [17]–[19]. In contrast to authentication or authorization, which regulates access rights, IM is intended to obscure the original data via linear mapping or transformation in such a way that only the executor can restore the actual data. With IM implemented, even if attackers have access to the information, they cannot obtain the real values. The greatest advantage of IM is not requiring additional devices or safety measures, and it can coexist with current authentication and authorization.

Alexander and Daniel [9], [10] investigated IM for the optimal power flow (OPF) problem by generating an entirely new OPF problem with different objective functions and constraints while preserving the power system structure. However, the requirement

Manuscript received November 29, 2016; revised February 28, 2017; accepted March 28, 2017. Date of publication April 12, 2017; date of current version October 19, 2018. This work was supported in part by the National Key Research and Development Program of China under Grant 2017YFB0903000 and in part by the U.S. Department of Energy (DOE)'s Office of Electricity Delivery and Energy Reliability under Contract DE-OE0000839. Paper no. TSG-01676-2016. *(Corresponding author: Qinglai Guo.)*

S. Xin, Q. Guo, H. Sun, and B. Zhang are with the Department of Electrical Engineering, State Key Laboratory of Power Systems, Tsinghua University, Beijing 100084, China (e-mail: xinsj14@mails.tsinghua.edu.cn; guoqinglai@tsinghua.edu.cn; shb@tsinghua.edu.cn; zhangbm@tsinghua.edu.cn).

C. Chen is with the Energy Systems Division, Argonne National Laboratory, Argonne, IL 60049 USA (e-mail: morningchen@anl.gov).

J. Wang is with the Department of Electrical Engineering, Southern Methodist University, Dallas, TX 75275 USA, and also with the Energy Systems Division, Argonne National Laboratory, Argonne, IL 60449 USA (e-mail: jianhui.wang@ieee.org).

This paper has supplementary downloadable multimedia material available at http://ieeexplore.ieee.org provided by the authors. This file includes the appendix "Further information on tools, algorithms and evaluation results." This material is 0.572 MB in size.

Color versions of one or more of the figures in this paper are available online at http://ieeexplore.ieee.org.

Digital Object Identifier 10.1109/TSG.2017.2693345

in [10] and [12] of knowing the optimal solutions for both the original and masked problems is sometimes hard to meet. In addition, for cloud-based EMS, an optimal problem may be generated from multiple sides and each part may need to be masked independently. Furthermore, the sparse property of the original power network matrix should also be preserved after IM. To sum up, for better feasibility and practical value of the IM technology, it is necessary to modify the approach with more reasonable assumptions as well as to integrally consider both privacy protection scenarios and computation requirements.

In this paper, we explore IM mechanisms for future cloud-based EMS. The main contributions of this paper are

- ➢ proposing IM mechanism for cloud-based EMS and specifically analyzing IM design rules for two general requirements;
- ➢ identifying the requirements of information protection and IM for three typical scenarios in future cloud-based EMSs;
- ➢ Proposing a construction-based IM approach as well as an implementation procedure for each scenario.

The remainder of this paper is organized as follows. In Section II, we review the basic model of IM. After summarizing two general requirements for IM, in Section III, we analyze their corresponding IM design rules. In Section IV, we briefly discuss the requirements and the rules of IM for the three typical cloud-based EMS scenarios. In Section V, we study three typical cases whose results verify the feasibility and effectiveness of our proposed IM approach. Section VI provides a summary and future outlook.

II. Basic Theory of IM

The essence of an EMS function is optimization based on current/historical information, where most constraints are linear (for example, DC OPF). Therefore, the key to IM is to equivalently transform the optimal function by hiding specified parameters or constants. Previous researchers have discussed the IM approach for a linear optimal function [9], [10]. In this section, we briefly review this method.

The standard form of a linear constrained optimal function is presented as follows:

$$\begin{aligned} \min\ & \frac{1}{2}x^T \cdot \boldsymbol{E} \cdot x + c^T \cdot x \\ s.t.\ & \boldsymbol{M}^{Eq} \cdot x = b^{Eq} \\ & \boldsymbol{M}^{IE} \cdot x + x^{sl} = b^{IE}\ x^{sl} \geq 0, \end{aligned} \tag{1}$$

where superscripts ^{Eq} and ^{IE} correspond to equality and inequality constraints. Slack variable x^{sl} is introduced for the inequality constraints. By expanding the original x, $\boldsymbol{E}$ and c to x', $\boldsymbol{E}$' and c', we reformulate the original function as:

$$\begin{aligned} \min\ & \frac{1}{2}x'^T \cdot \boldsymbol{E}' \cdot x' + c'^T \cdot x' \\ s.t.\ & \boldsymbol{M}' \cdot x' = b'\ \boldsymbol{I}'^{sl} \cdot x' \geq 0, \end{aligned} \tag{2}$$

whose parameters and constants are defined as follows:

$$\begin{aligned} & x' = \begin{bmatrix} x \\ x^{sl} \end{bmatrix},\ \boldsymbol{E}' = \begin{bmatrix} \boldsymbol{E} & 0 \\ 0 & 0 \end{bmatrix},\ c' = \begin{bmatrix} c \\ 0 \end{bmatrix} \\ & \boldsymbol{M}' = \begin{bmatrix} \boldsymbol{M}^{Eq} & 0 \\ \boldsymbol{M}^{IE} & \boldsymbol{I}^{sl} \end{bmatrix},\ b' = \begin{bmatrix} b^{Eq} \\ b^{IE} \end{bmatrix},\ \boldsymbol{I}'^{sl} = \begin{bmatrix} 0 & 0 \\ 0 & \boldsymbol{I}^{sl} \end{bmatrix}, \end{aligned} \tag{3}$$

in which matrix $\boldsymbol{I}^{sl}$ is a unit matrix corresponding to x^{sl}.

According to previous studies [9] and [10], we can use two random non-singular matrices $\boldsymbol{T}$ and $\boldsymbol{Q}$ and a random vector r to mask the optimal problem in equation (2). We define the following parameters and constants:

$$\begin{aligned} & \boldsymbol{F}' = \boldsymbol{Q}^T \cdot \boldsymbol{E}' \cdot \boldsymbol{Q} \quad a' = \boldsymbol{Q}^T \cdot c' - \boldsymbol{Q}^T \cdot \boldsymbol{E}' \cdot \boldsymbol{Q} \cdot r \\ & \boldsymbol{N}' = \boldsymbol{T} \cdot \boldsymbol{M}' \cdot \boldsymbol{Q} \quad d' = \boldsymbol{T} \cdot b' + \boldsymbol{N}' \cdot r, \end{aligned} \tag{4}$$

with which we can transform the original problem to:

$$\begin{aligned} \min\ & \frac{1}{2}z'^T \cdot \boldsymbol{F}' \cdot z' + a'^T \cdot z' \\ s.t.\ & \boldsymbol{N}' \cdot z' = d'\ \ \boldsymbol{I}'_{sl} \cdot \boldsymbol{Q} \cdot z' \geq \boldsymbol{I}'_{sl} \cdot \boldsymbol{Q} \cdot r \end{aligned} \tag{5}$$

Considering that additions or subtractions are not always applicable among inequalities, it is necessary to introduce slack variables to transform them to equalities before IM; thus, the scale of the masked problem (equation (5)) is unavoidably increased compared with the original one (equation (1)).

The relation between the optimal solutions of the original and masked problems, represented by x'^* and $\boldsymbol{z'^*}$, should always be:

$$x'^* = \begin{bmatrix} (x^*)^T & \left(x^{sl*}\right)^T \end{bmatrix}^T = \boldsymbol{Q} \cdot \left(z'^* - r\right), \tag{6}$$

with which we can accurately restore the real optimal solution x^* from the masked solution $\boldsymbol{z'^*}$.

A flow chart of IM in cloud computing is presented in Fig. 1, in which the original problems/results are labeled by a green box, and the IM procedure is labeled by a red box. The local-side and cloud-side processes are marked in light blue and light orange, respectively.

Instead of calculating an optimal problem (see the red dotted-line arrow at the bottom), the local side only implements IM, uploads the masked data to the cloud, and performs restoration after receiving the (masked) results. The complex optimal solution process, in contrast, is accomplished by the cloud based on only the masked data. Notably, only the local participants with full information of IM transformation, i.e., matrices $\boldsymbol{T}$ and $\boldsymbol{Q}$ and random vector r, could obtain the real solution. In this way, the local side can utilize the superior computation resources of the cloud side with its own information perfectly protected.

According to Fig. 1, the essence of IM is the linear mapping achieved by $\boldsymbol{T}$, $\boldsymbol{Q}$ and r, in which $\boldsymbol{Q}$ and r mask both the constraints and the solutions and $\boldsymbol{T}$ only masks the constraints. In theory, for any linear constrained problem, we can perform IM using any randomly selected $\boldsymbol{T}$, $\boldsymbol{Q}$ and r. However, real applications are usually restricted by numerous factors such as hardware condition and computation complexity. Therefore, in order to successfully implement IM theory in real cloud-based applications, it is necessary to answer the following three questions:

- ➢ What is the requirements for $\boldsymbol{T}$, $\boldsymbol{Q}$ and r?
- ➢ How to construct $\boldsymbol{T}$, $\boldsymbol{Q}$ and r?
- ➢ How the proposed IM mechanism can be implemented in real EMS applications?

In the following sections, we will first address two general requirements for IM applications in cloud-based EMS, then explore the three typical scenarios by answering the three abovementioned issues.

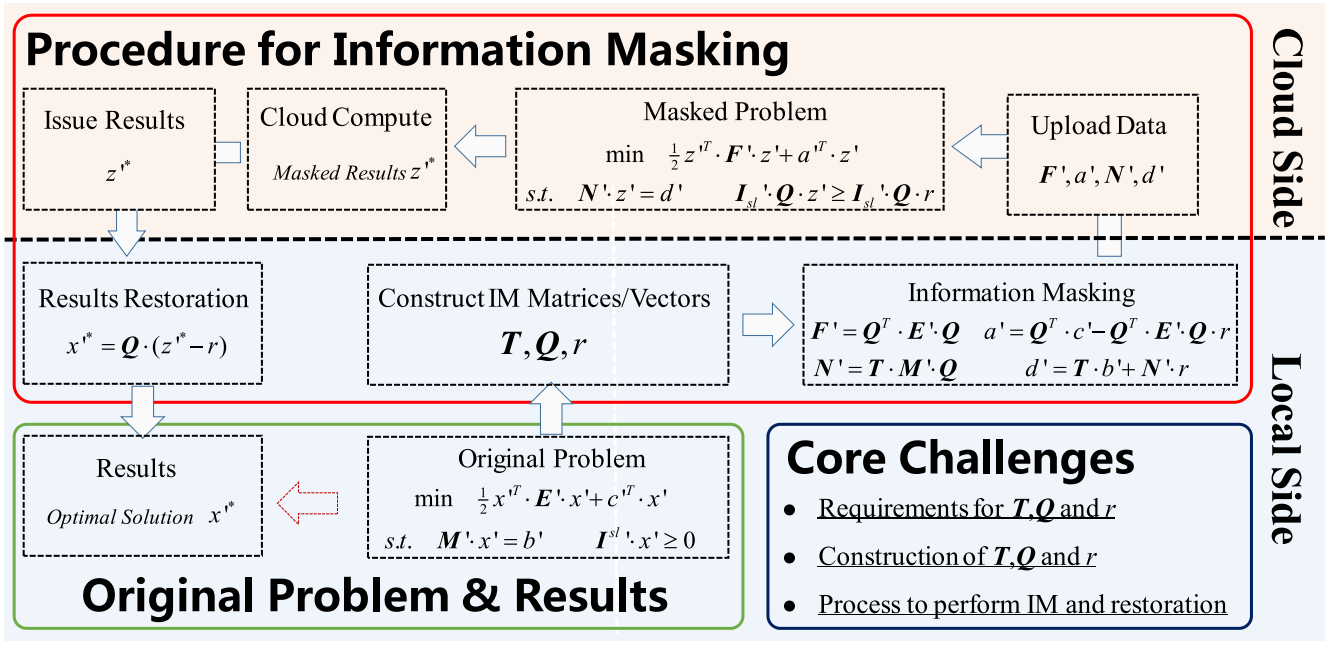

Fig. 1. A Brief Flow Chart of IM Application in Cloud Computing.

III. General Requirements for IM

Some current cloud-based EMS applications provide separate service for each independent user, while some may coordinately dispatch multiple participants' resources. In the latter scenario, an EMS function may have several independent information resources that need to be masked separately without affecting the others. Accordingly, we can summarize two core but general requirements for IM application in cloud-based EMSs, namely

- ➢ to preserve independence, which means that each participant masks its own information separately
- ➢ to preserve the partial model, which means that each participant's IM only hides its own information and does not modify the rest problem

To improve the practicability of IM methods in power system dispatching, in this section, we discuss how to generate $\boldsymbol{T}$, $\boldsymbol{Q}$ and r that satisfy these two general requirements.

A. Independence Preserving

Assume that there are n separate participants/units for the optimal dispatch in equation (2) whose constraints are

$$\boldsymbol{M}_i' \cdot x_i' = b_i', \ \boldsymbol{I}_{i,sl}' \cdot x_i' \geq 0 \quad 1 \leq i \leq n, \tag{7}$$

where i represents the participant/unit number. As IM processes can be regarded as linear mappings among constraints and variables, to preserve independence, each participant can only perform linear IM mappings among its own information; thus, $\boldsymbol{T}$, $\boldsymbol{Q}$ and r should be constructed in the following form:

$$\begin{aligned} &\boldsymbol{T} = diag(\boldsymbol{T}_1 \cdots \boldsymbol{T}_n), \ \boldsymbol{Q} = diag(\boldsymbol{Q}_1 \cdots \boldsymbol{Q}_n), \\ &r = \left[r_1^T \cdots r_n^T\right]^T, \end{aligned} \tag{8}$$

where $\boldsymbol{T}_i$, $\boldsymbol{Q}_i$ and r_i $(1 \leq i \leq n)$ are generated by the i^{th} participant.

Substituting equations (7) and (8) into (5), the masked constraints can be reformulated in the form of

$$\begin{aligned} &\boldsymbol{T}_i \cdot \boldsymbol{M}_i' \cdot \boldsymbol{Q}_i \cdot z_i' = \boldsymbol{T}_i \cdot b_i' + \boldsymbol{T}_i \cdot \boldsymbol{M}_i' \cdot \boldsymbol{Q}_i \cdot r_i \quad 1 \leq i \leq n \\ &\boldsymbol{I}_{i,sl}' \cdot \boldsymbol{Q}_i \cdot z_i' \geq \boldsymbol{I}_{i,sl}' \cdot \boldsymbol{Q}_i \cdot r_i, \end{aligned} \tag{9}$$

and each participant can restore its real solution by

$$x_i'^* = \left[x_i^{*T} \quad x_i^{sl*T}\right] = \boldsymbol{Q}_i \cdot \left(z_i'^* - r_i\right), \tag{10}$$

The detailed IM transformation for the entire problem is presented in Appendix A.

B. Partial Model Preserving

1) For the Objective Function: Considering that the introduction of a constant in the objective function should not affect the optimization result, according to equation (5), we only need to ensure

$$\boldsymbol{F}' = \boldsymbol{Q}^T \cdot \boldsymbol{E}' \cdot \boldsymbol{Q} = \boldsymbol{E}', a' = \boldsymbol{Q}^T \cdot c' - \boldsymbol{Q}^T \cdot \boldsymbol{E}' \cdot \boldsymbol{Q} \cdot r = c' \tag{11}$$

As matrix $\boldsymbol{F}'$ and $\boldsymbol{E}'$ are both symmetric, there exists a square matrix $\boldsymbol{G}$ that satisfies the condition

$$\boldsymbol{E}' = \boldsymbol{G}^T \cdot \boldsymbol{G} \tag{12}$$

The following is a sufficient condition for equation (12):

$$r \in Null(\boldsymbol{G}), \boldsymbol{Q} = \boldsymbol{I} + \boldsymbol{Q}' \text{ where } \boldsymbol{Q}' \subset Null\left(\left[\boldsymbol{G}^T, c'\right]^T\right), \tag{13}$$

where $\boldsymbol{I}$ is a unit matrix with the same size as $\boldsymbol{G}$.

2) For the Selected Constraints/Variables: First, we rewrite the original and masked problems in the following form

$$\begin{matrix} \min & f(x) \\ \left[\begin{matrix} \overline{\boldsymbol{M}^p} \\ \overline{\overline{\boldsymbol{M}^p}} \end{matrix} \quad \begin{matrix} \overline{\boldsymbol{M}^m} \\ \overline{\overline{\boldsymbol{M}^m}} \end{matrix}\right] \cdot \left[\begin{matrix} x^p \\ x^m \end{matrix}\right] = \left[\begin{matrix} \overline{b} \\ \overline{\overline{b}} \end{matrix}\right] \end{matrix} \quad \begin{matrix} \min & g(z) \\ \left[\begin{matrix} \overline{\boldsymbol{N}^p} \\ \overline{\overline{\boldsymbol{N}^p}} \end{matrix} \quad \begin{matrix} \overline{\boldsymbol{N}^m} \\ \overline{\overline{\boldsymbol{N}^m}} \end{matrix}\right] \cdot \left[\begin{matrix} z^p \\ z^m \end{matrix}\right] = \left[\begin{matrix} \overline{d} \\ \overline{\overline{d}} \end{matrix}\right], \end{matrix} \tag{14}$$

where superscript $^{m/p}$ corresponds to the masked/preserved variables, and superscript $^{=/-}$ corresponds to the masked/preserved constraints. Referring to this scenario, the IM transformation should meet the requirements below:

$$z^p = x^p, \overline{N^p} = \overline{M^p}, \overline{N^m} = \overline{M^m}, \bar{d} = \bar{b} \tag{15}$$

Here, we propose a construction method for $\boldsymbol{T}$, $\boldsymbol{Q}$ and r:

$$\boldsymbol{T} = \begin{bmatrix} \boldsymbol{I}^{-,-} & 0 \\ \boldsymbol{T}^{=,-} & \boldsymbol{T}^{=,=} \end{bmatrix}, \ \boldsymbol{Q} = \begin{bmatrix} \boldsymbol{I}^{p,p} & 0 \\ \boldsymbol{Q}^{p,m} & \boldsymbol{I}^{m,m} + \boldsymbol{Q}^{m,m} \end{bmatrix}, \quad \boldsymbol{r} = \begin{bmatrix} 0 \\ r^m \end{bmatrix}, \tag{16}$$

where superscripts $^{m/p}$ and $^{=/-}$ correspond to the elements in equation (14). $\boldsymbol{Q}^{p,m}$ and $\boldsymbol{Q}^{m,m}$ belong to the null space of matrix $\overline{M^m}$. $\boldsymbol{T}^{=,=}$ and $\boldsymbol{I}^{m,m} + \boldsymbol{Q}^{m,m}$ should be non-singular. This approach offers full flexibility in choosing r^m, $\boldsymbol{T}^{=,-}$ and $\boldsymbol{T}^{=,=}$ and some flexibility in selecting $\boldsymbol{Q}^{p,m}$ and $\boldsymbol{Q}^{m,m}$.

We define the set of all variables required to be preserved or occurring in the preserved model as x^o and define the rest as x^v. By specifying the null spaces of $\boldsymbol{G}$, $[\boldsymbol{G}^T, c]^T$ and $\overline{M^m}$, we can construct matrix $\boldsymbol{Q}$ in the following form:

$$\boldsymbol{Q} = \begin{bmatrix} \boldsymbol{I}^{o,o} & 0 \\ \boldsymbol{Q}^{o,v} & \boldsymbol{Q}^{v,v} \end{bmatrix}, \tag{17}$$

where $\boldsymbol{Q}^{v,v}$ is a random non-singular matrix. The side lengths of square matrices $\boldsymbol{I}^{o,o}$ and $\boldsymbol{Q}^{v,v}$ are, respectively, equal to the lengths of x^o and x^v.

3) For the Problem Scale (Constraint Quantity): The traditional IM approach offers a transformation mapping from the original problem (equation (1)) to a new one (equation (5)) [17]. However, considering that addition or subtraction cannot be directly implemented on inequality constraints, we introduce slack variables, which may seriously scale up the coefficient matrix by adding both constraints and variables. To preserve the scale of constraints and variables for better computation efficiency, we construct $\boldsymbol{T}$, $\boldsymbol{Q}$ and r for problem (1) in the following forms

$$\boldsymbol{T} = \begin{bmatrix} \boldsymbol{T}^{Eq,Eq} & 0 \\ \boldsymbol{T}^{IE,Eq} & \boldsymbol{T}^{IE,IE} \end{bmatrix}, \ \boldsymbol{Q} = \begin{bmatrix} \boldsymbol{Q}^{o} & 0 \\ 0 & \boldsymbol{Q}^{sl} \end{bmatrix}, \ r = \begin{bmatrix} r^{o} \\ r^{sl} \end{bmatrix}, \tag{18}$$

where $\boldsymbol{T}^{IE,IE}$ and $\boldsymbol{Q}^{sl}$ are random positive monomial matrices. Matrices $\boldsymbol{T}$ and $\boldsymbol{Q}$ should be non-singular.

After substituting equation (18) into (4), the masked problem in equation (5) can be simplified into the following equation (19), which retains the quantities of both the variables and the constraints after removing extra slack variables.

$$\begin{aligned} \min \ & \frac{1}{2} z^T \cdot \boldsymbol{F} \cdot z + a^T \cdot z \\ s.t. \ & \boldsymbol{N}^{Eq} \cdot z = d^{Eq} \ \ \boldsymbol{N}^{IE} \cdot z \le d^{IE} \end{aligned} \tag{19}$$

The original solution can be restored by

$$x^* = \boldsymbol{Q} \cdot \left(z^* - r\right) \tag{20}$$

See Appendix B, for the detailed IM transformation.

IV. IM Implementation in Cloud-Based EMSs

In the introduction, we have briefly introduced three typical levels of participants corresponding to three application scenarios for cloud-based EMSs. As discussed in the second section, the core to perform IM is to properly construct mapping matrices $\boldsymbol{T}$, $\boldsymbol{Q}$ and vector r. Therefore, in this section, we first analyze the model and IM requirements for the proposed EMS scenarios, then propose IM mechanisms and transformations for each scenario based on the theory discussed in Sections II and III. To link the theory with practice, an implementation method/procedure is presented at the end of the discussion.

A. IM Application for End Users: Cloud-Based Home/Building EMS

End users have become a new but essential category of participants in smart grids and may also expect to dispatch or optimize their own resources. Typical examples are smart homes and buildings. However, the current underlying customer-side terminals, such as smart meters, may not have enough calculation capacity for rolling optimization. Cloud computing, based on large storage and computational resources shared over the Internet, provides a feasible solution for this dilemma. A customer does not need to implement its own EMS locally. Instead, all the computing processes can be performed in the cloud by an EMS service vendor, and the local terminals only need to gather the local information and execute control [3], [4] after receiving commands from the cloud.

1) Service Function: The EMS services in this scenario are mainly designed for end users to help optimize and execute their electricity-consuming strategies, for example, minimizing the total electricity cost. A typical optimal model for a home EMS, which intends to minimize the total cost for electricity while satisfying all demands, is presented as follows:

$$\begin{aligned} \min \ & \sum_{t=1}^{m} c^t \cdot P_{\Sigma}^t && \ldots \text{Objective Function} \\ s.t. \ & P_{\Sigma}^t = \sum_{i=1}^{n} P_i^t, \underline{P_i^t} \le P_i^t \le \overline{P_i^t} \\ & \sum_{t=1}^{m} P_i^t = E_i, \underline{E_i^k} \le \sum_{t=1}^{k} P_i^t \le \overline{E_i^k}, \ \forall k, && \ldots \text{Power Constraints} \end{aligned} \tag{21}$$

where superscripts ^{t} and ^{i} represent the time and facility number, respectively; P and E refer to the power and energy of facilities; and c^t is the electricity price at time t. The overlines/underlines in equation (21) represent the upper/lower limits of the corresponding quantities. The parameters of the objective function, e.g., time-of-use electricity price c^t, are determined by electricity utilities and are publicly available. In contrast, the constraints, such as electricity demand and power limits, are private and are generated based on the information from the costumer side.

The constraints of the i^{th} component in problem (21) can be reformulated in the following form

$$\boldsymbol{M}_i^{Eq} \cdot \mathcal{P}_i = b_i^{Eq}, \boldsymbol{M}_i^{IE} \cdot \mathcal{P}_i \le b_i^{IE}, \tag{22}$$

where $\mathcal{P}_i$ is defined as $[P_i^{t=1}, \ldots, P_i^{t=m}]^T$ for any $1 \le i \le n$. Considering the modeling consistency of cloud-based computation, the structure of the constraints, i.e., coefficient matrices $\boldsymbol{M}_i^{Eq}$ and $\boldsymbol{M}_i^{IE}$, should be unified for a certain kind of component. In other words, the characteristics of component i are expressed by constant terms b_i^{Eq} and b_i^{IE} in equation (22). Therefore, local terminals only need to upload some constant values rather than entire constraints to reduce communication costs, with which the cloud server could still automatically generate the model based on the unified model.

2) Requirements of IM: In this scenario, both the device information and optimal plan need to be exchanged between the customer side and the cloud and are required to be masked to protect the customers' privacy [8]–[12]. However, the electricity price should not be changed. Therefore, the key challenge for this scenario's IM is to properly mask the local privacy, i.e., the constraints, without modifying the objective function, while ensuring the solvability of the original optimal problem.

In addition, as mentioned before, local terminals only need to upload constant terms b_i^{Eq} and b_i^{IE} to the cloud to reduce communication cost. Therefore, to preserve the uniformity of the constraints, coefficient matrices $\boldsymbol{M}_i^{Eq}$ and $\boldsymbol{M}_i^{IE}$, should be unchanged during IM.

Finally, the complexity of customer-level IM should also be controlled in consideration of the limitation of the data processing capacity of local terminals.

3) IM Mechanism: Referring to equation (22), to preserve uniformity, we can only mask b_i^{Eq} and b_i^{IE}, which correspond to $P_i^t, \overline{P_i^t}, E_i^k, \overline{E_i^k}$ and E_i in equation (21). Considering that $\boldsymbol{T}$ only masks the constraints, we set it as a unit matrix.

For $\boldsymbol{Q}$ and r, to preserve the uniformity, we introduce the idea of fabricating, i.e., fabricating several fictional same-type components for each component i to hide the original one.

We first generate an equivalent model for problem (21) with different quantities of components. Assume that component i is masked by l_i same-type components. After randomly selecting l_i positive quantities $\lambda_{i,1,\ldots,}\lambda_{i,li}$ whose sum is 1, we can equivalently transform the original problem (21) into the following form by creating l_i copies for each component i:

$$\begin{aligned}
&\min\ c^T \cdot \mathcal{P}_\Sigma \\
&s.t.\ \mathcal{P}_\Sigma = \sum_{i=1}^{n}\sum_{j=1}^{l_i} \lambda_{i,j} \cdot \mathcal{P}_{i,j} \\
&\quad \forall 1 \le i \le n \\
&\quad diag\left(\underbrace{\boldsymbol{M}_i^{Eq} \cdots \boldsymbol{M}_i^{Eq}}_{l_i}\right) \cdot \mathcal{P}_i^{copy} = \underbrace{\left[\left(b_i^{Eq}\right)^T \cdots \left(b_i^{Eq}\right)^T\right]}_{l_i} \\
&\quad diag\left(\underbrace{\boldsymbol{M}_i^{IE} \cdots \boldsymbol{M}_i^{IE}}_{l_i}\right) \cdot \mathcal{P}_i^{copy} \le \underbrace{\left[\left(b_i^{IE}\right)^T \cdots \left(b_i^{IE}\right)^T\right]}_{l_i}
\end{aligned} \tag{23}$$

where $\mathcal{P}_\Sigma$ is defined as $[P_\Sigma^{t=1}, \ldots, P_\Sigma^{t=m}]^T$, and $\mathcal{P}_i^{copy}$ is defined as $[\mathcal{P}_{i,1}^T \cdots \mathcal{P}_{i,l_i}^T]^T$ for each $1 \le i \le n$. Here $\mathcal{P}_{i,j}$ represents the power of the j^{th} copy of the i^{th} component $(1 \le j \le l_i)$. After comparing the solutions of problems (21) and (23), we have:

$$\mathcal{P}_i^* = \sum_{j=1}^{l_i} \lambda_{i,j} \cdot \mathcal{P}_{i,j}^* \tag{24}$$

Then, we perform IM on the equivalent model. Defining $\mathcal{P} = [(\mathcal{P}_\Sigma)^T, (\mathcal{P}_1^{copy})^T \cdots (\mathcal{P}_n^{copy})^T]^T$, we construct

$$\begin{aligned}
\boldsymbol{Q} &= diag\left(\boldsymbol{I}_\Sigma, \boldsymbol{Q}_1^{copy}, \ldots, \boldsymbol{Q}_n^{copy}\right), \\
r &= \left[0, \left(r_1^{copy}\right)^T, \ldots, \left(r_n^{copy}\right)^T\right]^T,
\end{aligned} \tag{25}$$

where

$$\boldsymbol{Q}_i^{copy} = diag\left(1/\lambda_{i,1} \cdot \boldsymbol{I}_i \cdots 1/\lambda_{i,l_i} \cdot \boldsymbol{I}_i\right), r_i^{copy} = \left[r_{i,1}^T \cdots r_{i,l_i}^T\right]^T, \tag{26}$$

for each $1 \le i \le n$. As the form of $\boldsymbol{Q}$ satisfies the requirement in equation (17), the objective function can be retained. In addition, $\lambda_{i,1,\ldots,}\lambda_{i,li}$ and $r_{i,1,\ldots,}r_{i,li}$ are randomly selected variables, so equation (24) offers enough flexibility in determining $\boldsymbol{Q}$ and r.

After substituting equation (25) into (5), we obtain:

$$\begin{aligned}
&\min\ c^T \cdot \mathcal{Z}_\Sigma \\
&s.t.\ \mathcal{Z}_\Sigma = \sum_{i=1}^{n}\sum_{j=1}^{l_i} \mathcal{Z}_{i,j} \\
&\quad \forall 1 \le i \le n,\ \forall 1 \le j \le l_i \\
&\quad \boldsymbol{M}_i^{Eq} \cdot \mathcal{Z}_{i,j} = \lambda_{i,j} \cdot b_i^{Eq} + \boldsymbol{M}_i^{Eq} \cdot r_{i,j} \\
&\quad \boldsymbol{M}_i^{IE} \cdot \mathcal{Z}_{i,j} \le \lambda_{i,j} \cdot b_i^{IE} + \boldsymbol{M}_i^{IE} \cdot r_{i,j}
\end{aligned} \tag{27}$$

which preserves the uniformity of the constraints. The relation between the masked and real solutions should always be:

$$\mathcal{P}_i = \sum_{j=1}^{l_i} \lambda_{i,j} \cdot \mathcal{P}_{i,j} = \sum_{j=1}^{l_i} \mathcal{Z}_{i,j} - \sum_{j=1}^{l_i} r_{i,j} \quad \forall 1 \le i \le n. \tag{28}$$

4) Implementation Method: According to the proposed mechanism, each smart device is able to hide its own information independently. The operation procedure of IM in customer-side applications is proposed as follows:

a. When installing EMS service to the cloud, classify all the smart devices and generate the standard model for each category;
b. For each customer-side device, preset its constraint information b_i^{Eq} and b_i^{IE} (see equation (22) for definition) in its embedded smart chips;
c. For each embedded smart chip, select l_i positive quantities $\lambda_{i,1,\ldots,}\lambda_{i,li}$ whose sum is 1, and randomly select l_i quantities $r_{i,1,\ldots,}r_{i,li}$, then calculate

$$\begin{aligned}
&\forall 1 \le j \le l_i \\
&b_{i,j}^{Eq} = \lambda_{i,j} \cdot b_i^{Eq} + \boldsymbol{M}_i^{Eq} \cdot r_{i,j}, \\
&b_{i,j}^{IE} = \lambda_{i,j} \cdot b_i^{IE} + \boldsymbol{M}_i^{IE} \cdot r_{i,j}
\end{aligned} \tag{29}$$

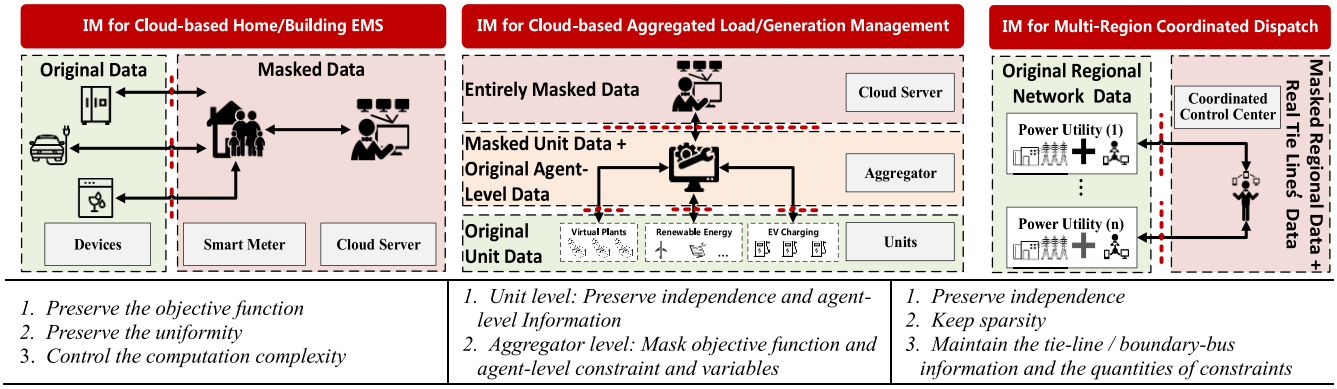

Fig. 2. IM Application Methods and Information Flows in Three Scenarios.

so that customer-side smart meter only gathers the masked information b_i^{Eq} and $b_i^{IE}(1 \le j \le l_i)$;

d. After receiving the masked information, the cloud-side EMS automatically generate the optimization problem in equation (27) according to the preset standard model, and solve it afterwards;

e. Issue the masked solution $\mathcal{P}_{i,j}^*(1 \le i \le n, 1 \le j \le l_i)$ to the local side;

f. After receiving the masked results, each embedded smart chip restore the original solution with equation (28).

In real applications, rather than performing the entire IM process, i.e., constructing $\boldsymbol{T}$, $\boldsymbol{Q}$ and r and mask the entire problem, the local terminals only needs to select proper $\lambda_{i,1,\ldots},\lambda_{i,li}$ and $r_{i,1,\ldots},r_{i,li}$ and then calculate the constant terms utilizing equation (29). In this way, the IM can be executed by simple additions and multiplications; thus, the complexity should be acceptable. To clearly illustrate the IM application method, we present the information flow in Fig. 2, in which each bold dotted red line represents a separate IM process.

B. IM Application for Agents: Cloud-Based Aggregated Load/Generation Management

The introduction of ICTs has enabled a regional controller to take advantage of mass but low-capacity components within the region, such as EV charging loads, demand response facilities, distributed generators, and virtual plants, even though they may be owned by different units. A typical example is the optimal load and energy storage dispatch for an industrial park or a residential area in the form of aggregator. However, sometimes it is impossible to directly deploy or maintain a separate EMS for each aggregator because of its extremely high cost and inconvenience. In this respect, cloud computing, which offers extra external computation and communication resources, is envisaged as a core technology for remote deployment and maintenance [3], [4].

1) Service Function: The facilities within a region, such as EV parking lots and virtual plants, may be owned by different independent individuals or units, and they are dispatched by one aggregator. Under normal conditions, the constraints for Scenario 2 can be divided into two levels: agent level, which represents the constraints of the regional system, and unit level, which represents the constraints of independent units/facilities. A standard form of the optimal model is presented as follows:

$$\begin{aligned} \min\ & \tfrac{1}{2}\left(P'_\Sigma\right)^T \cdot \boldsymbol{E}' \cdot P'_\Sigma + c'^T \cdot P'_\Sigma \qquad \ldots \text{Objective Function} \\ s.t.\ & \boldsymbol{M}'_\Sigma \cdot P'_\Sigma = b'_\Sigma\ P'_\Sigma = \left[P_{1,\sum} \cdots P_{n,\sum}, P_\Sigma^{sl}\right]^T, \\ & \qquad \ldots \text{Agent} - \text{Level Constraints} \\ & 1 \le i \le n\ \boldsymbol{M}'_i \cdot x'_i = b'_i\ x_i = \left[P_{i,\sum}, u_i^T, u_i^{slT}\right]^T \\ & \qquad \ldots \text{Unit} - \text{Level Constraints} \end{aligned} \tag{30}$$

where subscript $_i$ represents the facility number; and superscript ^{sl} refers to slack variables. For facility i, only $P_{i,\Sigma}$, which represents its total power consumption, should be accurately obtained by the aggregator, while the remaining private operation data u_i need to be protected. Take an EV charging station as an example: u_i may include information about the charging power, arrival/departure time and SOC (state of charge) for all its controlled poles/EVs.

2) Requirements of IM: The objective function and agent-level constraints are determined by the aggregator, and the unit-level constraints are generated separately by each unit. Therefore, there are two types of data exchange processes in this scenario: between the facilities and the aggregator, in which the aggregator gathers the facility constraints and issues the optimal plan, and between the aggregator and the cloud server, in which the aggregator uploads the entire model and receives the cloud-computed results. Accordingly, we need to generate two groups of $\boldsymbol{T}$, $\boldsymbol{Q}$ and r for the two levels of IMs:

- ➢ At the unit/facility level, the IM is performed independently by each unit; thus, the goal is to design a local-information-based mechanism that does not affect the agent-level constraints or the objective function.
- ➢ At the aggregator level, as the facility constraints have been masked perfectly by each unit, the IM should especially be focused on the objective function as well as the agent-level constraints.

3) IM Mechanism: The IM mechanism for this scenario should be designed for both the aggregator and the units.

a) Unit-level IM: The key requirement for the unit-level IM is that it should be performed independently by each unit while does not affect the agent-level information.

To satisfy this requirement, according to equation (8), we generate the IM mapping in the following form:

$$\boldsymbol{T} = diag(\boldsymbol{T}_a, \boldsymbol{T}_1 \cdots T_n), \boldsymbol{Q} = diag\big(\boldsymbol{Q}_1 \cdots \boldsymbol{Q}_n\big),$$
$$r = \left[r_1^T \cdots r_n^T\right]^T, \tag{31}$$

where subscripts $_a$ and $_{1 \ldots n}$ correspond to agent-level constraints and facility constraints, respectively.

According to equation (30), for each unit $i(1 \le i \le n)$, only $P_{i,\Sigma}$ occurs in the agent-level constraints and the objective function. To preserve them, we construct $\boldsymbol{T}_{\mathrm{a}}$, $\boldsymbol{Q}_i$ and r_i in the following form based on equations (16) and (17)

$$\boldsymbol{T}_a = \boldsymbol{I}_a, \boldsymbol{Q}_i = \begin{bmatrix} \boldsymbol{I}_i^{P_\Sigma, P_\Sigma} & 0 \\ \boldsymbol{Q}_i^{P_\Sigma, m} & \boldsymbol{Q}_i^{m,m} \end{bmatrix}, r_i = \begin{bmatrix} 0 \\ r_i^m \end{bmatrix}, \tag{32}$$

where $\boldsymbol{I}$ represents a unit matrix, and $\boldsymbol{Q}_i^{m,m}$ is a random non-singular matrix. The side lengths of $\boldsymbol{I}_i^{P_\Sigma, P_\Sigma}$ and $\boldsymbol{Q}_i^{m,m}$ are equal to $length(P_{i,\Sigma})$ and $length(u_i + u_i^{sl})$, respectively. This approach offers enough flexibility in choosing $\boldsymbol{T}$, $\boldsymbol{Q}$ and r.

b) Aggregator-level IM: The aggregator has full information about the whole problem; thus, it can perform IM with arbitrary $\boldsymbol{T}$, $\boldsymbol{Q}$ and r. However, as each unit has masked its local information already, the aggregator only needs to mask the rest, i.e., the objective function and the agent-level constraints. $\boldsymbol{T}$, $\boldsymbol{Q}$ and r can be constructed based on equations (14)-(17).

4) Implementation Method: The operation procedure for agent-level EMS applications is proposed as follows:

a. For each local unit $i(1 \le i \le n)$, construct $\boldsymbol{Q}_i$ and r_i in the form proposed in equation (32), and randomly generate a square matrix $\boldsymbol{T}_i$;
b. The information of each unit i (see equation (30)) can be masked in the following form:

$$\boldsymbol{T}_i \cdot \boldsymbol{M}_i' \cdot \begin{bmatrix} P_{i,\Sigma} \\ \eta_i' \end{bmatrix} = \boldsymbol{T}_i \cdot b_i' + \boldsymbol{T}_i \cdot \boldsymbol{M}_i' \cdot \boldsymbol{Q}_i \cdot r_i, \tag{33}$$

in which η_i' represents the masked variables corresponding to u_i^T and u_i^{sl}. Obviously, the variables occurring in the agent-level constraints, i.e., $P_{i,\Sigma}$, is preserved.
c. After obtaining the masked constraints from each unit, the aggregator can perform IM on the entire problem (see equation (30)) with arbitrary $\boldsymbol{T}$, $\boldsymbol{Q}$ and r, then uploads the masked problem to the cloud server;
d. After receiving the solution from the cloud server, the aggregator restores the results using equation (6), then issues $P_{i,\sum}$ and η_i' to each unit;
e. Each unit could obtain its corresponding optimal solution using the following equation

$$u_i = \boldsymbol{Q}_i^{P_\Sigma, m} \cdot P_{i,\sum} + \boldsymbol{Q}_i^{m,m} \cdot \left(\eta_i' - r_i^m\right), \tag{34}$$

in which $\boldsymbol{Q}_i^{P_\Sigma, m}$ and $\boldsymbol{Q}_i^{m,m}$ are the sub-matrices of $\boldsymbol{Q}_i$ that are defined in equation (32).

C. IM Application for Interconnected Power Network: Cloud-Based Coordinated Dispatch for Multi-Regional Power Systems

Multi-area interconnection has become an essential trend for future power systems, in which global optimizations could obtain better economy and higher efficiency for the whole system than local optimization. Considering that different regions may be owned and operated by different corporations, some researchers have designed distributed approaches for such coordinated decisions in which each region locally computes and exchanges selected results with adjacent regions [21]. Such distributed approaches protect the privacy of each region and reduce the computation of each server but may seriously increase communication costs because of the iterative data interaction among different regions. Therefore, if an independent trusted-third-party could offer cloud-based EMS service to perform and issue the optimal decision for all regions, a centralized decision method may be possible and acceptable. However, the data protection issue for each region should be addressed.

1) Service Function: DC OPF is a typical category of power system dispatch functions, the standard form of which is presented as follows:

$$\begin{aligned} \min \ & \tfrac{1}{2} P^T \cdot \boldsymbol{E} \cdot P + c^T \cdot P && \ldots \text{Objective Function} \\ s.t. \ & -P^g + \boldsymbol{B} \cdot \theta = P^L \\ & -\overline{P^{line}} \le diag\left(b^{br}\right) \cdot \boldsymbol{A}^T \cdot \theta \le \overline{P^{line}} && \ldots \text{DC Flow Constraints} \\ & \boldsymbol{P}_{g,\min} \le j \le \boldsymbol{P}_{g,\max} && \ldots \text{Generation Constraints} \end{aligned} \tag{35}$$

In this model, P and θ represent the bus loads and bus voltage angles, respectively. Superscripts ^{line}, ^{L} and ^{g} represent the transmission line, load and generator. For the coefficients, matrix $\boldsymbol{B}$ is the imaginary part of the node susceptance matrix, b^{br} contains the branch susceptances, $diag\ (b^{br})$ is the diagonal matrix with the vector b^{br} on the diagonal, and matrix $\boldsymbol{A}$ is the node-branch incidence matrix. $\boldsymbol{B}$ is typically sparse.

The standard form of a multi-region coordinated dispatch is similar to equation (35). The only difference is that there are multiple separate sub-networks connected by tie lines and the tie-line flows are required to be scheduled in advance. Defining the set of the numbers for the tie lines between connected regions J_1 and J_2 as $\Psi(J_1, J_2)$, the tie-line schedule constraints can be manifested in the form below:

$$\underline{P_{J_1,J_2}^{tie}} \le P_{J_1,J_2}^{tie} = \sum_{k \in \Psi(J_1,J_2)} b_k^{br} \cdot \left(\theta_{k \cap J_1} - \theta_{k \cap J_2}\right) \le \overline{P_{J_1,J_2}^{tie}}. \tag{36}$$

2) Requirements of IM: In this scenario, regional power systems may be owned and operated by different corporations. For a corporation, its network data is a crucial commercial secret that needs to be protected. Therefore, each corporation implements IM independently and separately.

As the external characteristics of a regional network to the outside are reflected by the tie lines it relates to, a significant feature of this scenario is that the tie-line constraints (see equation 36) should be real and public. Therefore, the constraints and variables in equation (35), as well as the elements in $\boldsymbol{B}$ and $diag(b_{br}) \cdot \boldsymbol{A}^T$, that correspond to tie lines are required to be preserved after IM. In addition, for better communication

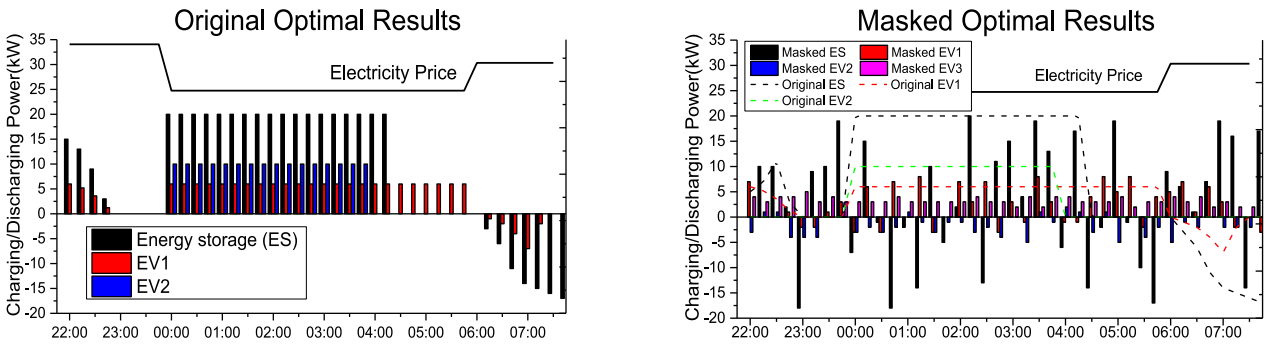

Fig. 3. Comparison between the Original and Masked Results.

and computation efficiency, it is also necessary to maintain the quantities of variables and constraints (rather than increase them) and to control the matrix sparsity.

3) IM Mechanism: The key challenge of the IM for this scenario is to properly hide the power network information, i.e., to mask the DC flow constraints in equations (35) and (36). According to the right graph in Fig. 2, IM for this scenario should be performed separately by each region and needs to preserve both the independence and sparsity. For brevity, we only discuss the mechanism to construct $\boldsymbol{Q}$ and r, which can mask all the information. If necessary, we can similarly construct matrix $\boldsymbol{T}$ by referring to $\boldsymbol{Q}$'s construction mechanism.

To preserve the independence, we should construct $\boldsymbol{Q}$ and r in the following form:

$$\boldsymbol{Q} = diag(\boldsymbol{Q}_1 \dots \boldsymbol{Q}_n),\ r = \left[r_1^T \dots r_n^T\right]^T \tag{37}$$

where subscripts $_{1\dots n}$ correspond to different regions. Hereafter, we discuss how each region i constructs $\boldsymbol{Q}_i$ and r_i.

From the perspective of a given sub-network J_i, the constraints of a coordinated dispatch problem (see equations (35) and (36)) can be reformulated in the following form:

$$\begin{aligned}
&\begin{matrix} I \\ B \\ E \end{matrix}\begin{bmatrix} B_{J_i}^{II} & B_{J_i}^{IB} & 0 \\ B_{J_i}^{BI} & B_{J_i}^{BB} & B_{J_i}^{BE} \\ 0 & B_{J_i}^{EB} & B_{J_i}^{EE} \end{bmatrix}\begin{bmatrix} \theta_{J_i}^{I} \\ \theta_{J_i}^{B} \\ \theta_{J_i}^{E} \end{bmatrix} = \begin{bmatrix} P_{J_i}^{L(I)} \\ P_{J_i}^{L(B)} \\ P_{J_i}^{L(E)} \end{bmatrix} - \begin{bmatrix} P_{J_i}^{g(I)} \\ P_{J_i}^{g(B)} \\ P_{J_i}^{g(E)} \end{bmatrix} \\
&abs\left(diag\left(b_{J_i}^{line(I\cup B)}\right)\cdot\left(A_{J_i}^{line(I\cup B)}\right)^T\cdot\begin{bmatrix}\theta_{J_i}^{I}\\ \theta_{J_i}^{B}\end{bmatrix}\right) \le \overline{P_{J_i}^{line(I\cup B)}} \\
&\forall \Psi(J_i,J_j)\neq\emptyset,\ abs\left(\sum_{k\in\Psi(J_i,J_j)} b_k^{br}\cdot\left(\theta_{k\cap J_i}-\theta_{k\cap J_j}\right)\right) \le \overline{P_{J_i,J_j}^{tie}},
\end{aligned} \tag{38}$$

where $abs()$ is the absolute function. Specifically, we label the internal/boundary/external node set with superscript $^{I}/^{B}/^{E}$.

In equation (38), the local information includes $B_{J_i}^{II}$, $B_{J_i}^{IB}$, $B_{J_i}^{BI}$, $B_{J_i}^{BB}$, $\theta_{J_i}^{I}$, $\theta_{J_i}^{B}$, $P_{J_i}^{L(B)}$, $P_{J_i}^{L(I)}$, $P_{J_i}^{g(I)}$, $P_{J_i}^{g(B)}$, $b_{J_i}^{line(I\cup B)}$ and $A_{J_i}^{line(I\cup B)}$, and the public or other regions' information refers to the rest. Notably, the external characteristics of J_i are represented by the voltage angles of its boundary nodes, $\theta_{J_i}^{B}$. Therefore, even though $\theta_{J_i}^{B}$ belongs to the local information, it should also be preserved during IM. In general, the goal for constructing $\boldsymbol{Q}_i$ and r_i is to mask only the above-mentioned local information except $\theta_{J_i}^{B}$ while preserving the rest.

TABLE I
PARAMETERS OF THE HOME FACILITIES

	Energy Storage	EV1	EV2
Electricity Capacity	100 kWh	40 kWh	50 kWh
Charging Power (max)	20 kW	6 kW	10 kW
Discharging Power (max)	20 kW	6 kW	0
Current SOC	20%	20%	10%
Target SOC	–	90%	90%
Departure Time	–	6:00 am	5:30 am

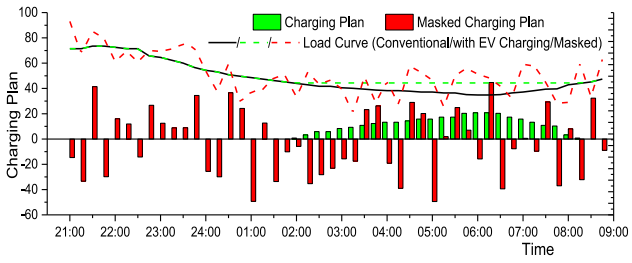

Fig. 4. Comparison between the Real and Masked Charging Plan.

After deliberation on sparsity, we propose a construction method for $\boldsymbol{Q}_i$ and r_i referring to equations (11)-(20):

a. Sort region i's internal node degrees from small to large;
b. Traverse all its internal and boundary nodes to generate a tree and introduce an external node as its root, such that 1) all the boundary nodes are leaves and 2) the internal nodes' degrees in the new tree are in reverse order to those in the original sub-network;
c. Generate node-branch incidence matrix $\boldsymbol{A}_{J_i}^{Tr(I\cup B)}$ for the tree by setting the introduced external node as the reference node. After properly sorting all the branches, the form of the generated matrix can be:

$$\boldsymbol{A}_{J_i}^{Tr(I\cup B)} = \begin{bmatrix} \boldsymbol{A}_{J_i}^{Tr(II)} & \boldsymbol{A}_{J_i}^{Tr(IB)} \\ 0 & \boldsymbol{I}_{J_i}^{BB} \end{bmatrix}, \tag{39}$$

where superscripts ^{I} and ^{B} correspond to internal and boundary nodes, respectively;
d. $\boldsymbol{Q}_i$ and r_i can be generated as follows:

$$\boldsymbol{Q}_i = abs\left(\boldsymbol{A}_{J_i}^{Tr(I\cup B)}\right),\ r_i = \begin{bmatrix}\left(\delta^I\right)^T & 0\end{bmatrix}^T \tag{40}$$

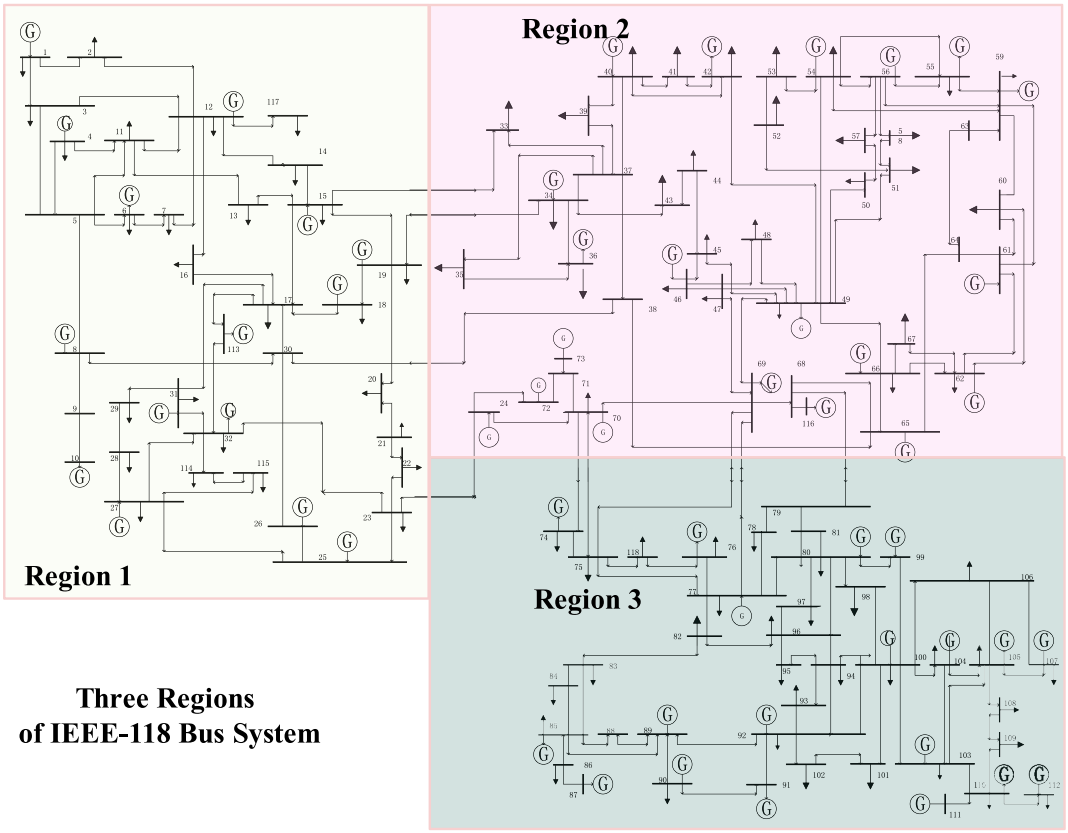

Fig. 5. The network structure and regions of the IEEE 118-bus system.

In this way, the local information of sub-network J_i can be masked into the following form:

$$\begin{aligned} \boldsymbol{B}_{J_i}^{I\cup B} &\rightarrow \boldsymbol{B}_{J_i}^{I\cup B}\cdot\boldsymbol{Q_i} \\ \left(b_{J_i}^{line(I\cup B)}\right)\cdot\left(\boldsymbol{A}_{J_i}^{line(I\cup B)}\right)^T &\rightarrow \left(b_{J_i}^{line(I\cup B)}\right)\cdot\left(\boldsymbol{A}_{J_i}^{line(I\cup B)}\right)^T\cdot\boldsymbol{Q_i} \end{aligned} \tag{41}$$

In equation (40), although each tree corresponds to only one matrix $\boldsymbol{Q}_i$, there is enough flexibility in generating the tree. In addition, equation (40) offers full flexibility for δ^I. With respect to the impact on computation efficiency, we prove that the sparsities of the masked coefficient matrices should be no more than twice the original values in Appendix C. The case study results verify that this increase does not affect the computation efficiency.

To clearly illustrate the proposed three scenarios and their information flows for IM, we give a brief comparison in Fig. 2, in which each bold dotted red line represents a separate IM process.

V. Case Study

In this section, we propose three cases to demonstrate the effectiveness of the IMs designed for the three EMS scenarios.

A. Scenario 1: Cloud-Based Home EMS

For customer-level IM, we take a cloud-based home EMS as an example. Assume that a house has an energy storage device and two EVs, whose parameters are presented in Table I.

In this condition, the cloud server generates an optimal plan for the three devices. To protect residential privacy, we introduce customer-level IM to hide the local information, in which a new house model with one energy storage device and three EVs is fabricated according to the proposed mechanism. The comparison between the original and masked operation plan for the next 40 time intervals is presented in Fig. 3.

According to the graphs, there are significant differences between the original and masked plans, and the plan restored from the masked results is the same as the original (see the dashed lines in the right graph). Both verify the effectiveness of our IM approach. In addition, its negligible computation cost (288 additions and 192 multiplications for this case) makes the IM feasible for smart chips. Therefore, this approach is highly applicable to future smart home facilities without requiring extra facilities or devices.

B. Scenario 2: Aggregated EV Optimal Charging

For system-level IM, we study a case of EV optimal charging dispatch. We do not consider the power network, whose IM will be discussed in detail in the next subsection. A standard model of an optimal valley-filling charging dispatch for multiple EV clusters, such as parking lots/charging stations, is presented below, where superscript ^{i} represents the number of the EV cluster, n is the number of the EV, and $r_n^i(\tau)$ represents

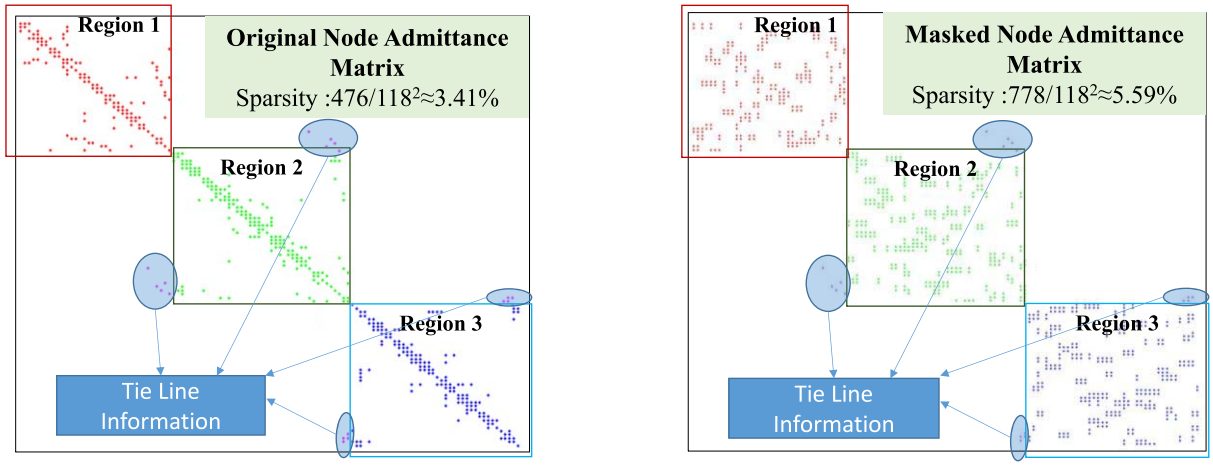

Fig. 6. Non-zero elements' distributions in the original and masked coefficient matrices.

the charging power of the n^{th} EV of the i^{th} cluster at time τ.

$$\begin{aligned} \min \ & \sum_{\tau\in\mathcal{T}_t}\left(\sum_i\left(P^i(\tau)+D^i(\tau)\right)\right)^2 \\ s.t. \ & P^i(\tau)=\sum_{n\in\mathcal{N}_t^i} r_n^i(\tau), \sum_{\tau\in\mathcal{T}_t} r_n(\tau)\Delta t = R_n^i \\ & 0\le r_n^i(\tau)\le \bar{r}_n^i(\tau), \tau\in\mathcal{T}_t, n\in\mathcal{N}_t^i \end{aligned} \tag{42}$$

Each unit (i.e., EV cluster) and the aggregator can mask its own information using the method discussed in Section IV In this case, the conventional loads and EVs are set based on reference [22]. In our study, the optimal charging decisions with and without IM are computed in 13.76 s and 14.6 s, respectively, which verifies the efficiency of our IM approach. The real and masked charging plans are compared in Fig. 4.

The results show that both the optimal charging dispatches with and without IM can achieve load shifting, but the masked results are significantly different from the real ones. Although the dispatch with IM and restoration consumes slightly more time (14.6 s compared with 13.76 s), this acceptable extra computation time of less than one second allows successful masking of all the local constraints and operation information.

C. Scenario 3: Coordinated Dispatch for Multi-Regional Power System

In this section, we study a generation dispatch problem for an IEEE 118-bus system to demonstrate how our IM approach masks the network information for each region. The network structure and its divisions into regions are presented in Fig. 5.

According to Fig. 5, the boundary buses of the three regions are, respectively, $\Omega_1 = \{15, 19, 30, 23\}$, $\Omega_2 = \{24, 33, 34, 38, 69, 70\}$ and $\Omega_3 = \{74, 75, 77, 79\}$. When IM is applied, each region hides its local information using the transformation process discussed in Section IV-C.

The cloud-side dispatch center generates multi-network constraints after receiving information from each region. The non-zero elements' distributions in the coefficient matrices (node susceptance matrix) of the DC power flow constraints

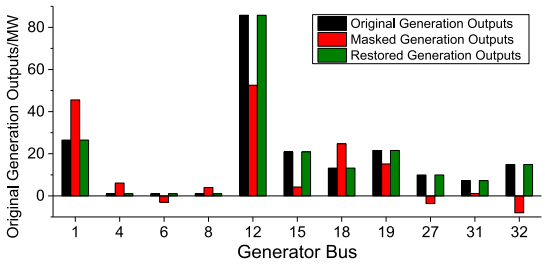

Fig. 7. The Original, Masked and Restored Generation Outputs in Region 1.

TABLE II
COMPARISON BETWEEN THE ORIGINAL AND MASKED PROBLEM

Computation Time	5.48 s (compared with 5.1 s)
Average Difference in Regional Information	>300%
Average Difference in Generator Outputs	>100%
Difference Between Real and Restored Results	0

with and without IM are compared in Fig. 6, and a brief comparison of the original and masked problem/results is proposed in Table II. To better illustrate the effectiveness of the IM approach, we compare the original, masked and restored output plans for some generators in Region 1 in Fig. 7.

The results computed with masked information can be exactly restored to the original values, which verifies the correctness of the IM approach. In addition, three points deserve special attention in Fig. 6: a) there are significant differences between the non-zero elements' distributions in two matrices; b) the boundary-node information (elements' locations and values, which are labeled by blue boxes in Fig. 6) has not been changed; and c) the original block-divided feature is preserved because each region performs IM independently. With these convincing results, the effectiveness and feasibility of IM application in cloud-based coordinated dispatch for multi-regional power systems can be verified.

Admittedly, according to Fig. 6, the sparsity has been increased from 3.41% to 5.59% because of IM, but it only leads to less than a 0.4 s increase in computation time. Therefore, this minor sacrifice of computation efficiency is acceptable for information isolation and privacy protection.

VI. Conclusion

Cloud-based dispatch has become an essential trend for future EMS design because of its high compatibility for mass quantities/types of participants. However, its unavoidable information exchange raises concern about information protection. Therefore, we have discussed the mechanisms of IM and its applications in three typical scenarios of cloud-based EMSs that serve three typical categories of participants, i.e., end user, agent and interconnected power network. By transforming the original data to another group of data, IM helps to obscure private information without affecting the decision of an EMS.

There are two core but general challenges for IM implementation. One is to preserve independence or how different units mask their own information independently. The other is to preserve the partial model when there are multiple information resources for an EMS function so that each participant's IM does not affect the others. In addition, some other factors, such as sparsity and complexity, may also need to be considered when designing IM for some EMS scenarios.

As an effective supplement to current privacy-related authentication and authorization approaches, IM does not require extra safety measures and is thus highly applicable. The research in this paper can be regarded as a step towards the implementation of information security and privacy protection in future cloud-based EMSs. Future work on this topic would investigate IM methods for nonlinear constraints.

Appendix A

IM Transformation for Preserving Independence

In equation (2), as matrix $\boldsymbol{E'}$ is symmetric, there exists a square matrix $\boldsymbol{G}$ that satisfies the condition

$$\boldsymbol{E}' = \boldsymbol{G}^T \cdot \boldsymbol{G}$$

Define

$$\boldsymbol{G} = [\boldsymbol{G}_1 \cdots \boldsymbol{G}_n],\ x' = \left[\left(x'_1\right)^T \cdots \left(x'_n\right)^T\right]^T$$
$$c' = \left[\left(c'_1\right)^T \cdots \left(c'_n\right)^T\right]^T$$

The original function can be reformulated as

$$\frac{1}{2}\left(\sum_{i=1}^{n} \boldsymbol{G}_i \cdot x'_i\right)^T \cdot \left(\sum_{i=1}^{n} \boldsymbol{G}_i \cdot x'_i\right) + \sum_{i=1}^{n} \left(c'_i\right)^T \cdot x'_i$$
$$s.t.\ \boldsymbol{M}'_i \cdot x'_i = b'_i,\ \boldsymbol{I}'_{i,sl} \cdot x'_i \geq 0, 1 \leq i \leq n,$$

After substituting equations (12) and (13) into (5), the masked problem can be expressed as

$$\frac{1}{2}\left(\sum_{i=1}^{n} \boldsymbol{G}_i \cdot \boldsymbol{Q}_i \cdot z'_i\right)^T \cdot \left(\sum_{i=1}^{n} \boldsymbol{G}_i \cdot \boldsymbol{Q}_i \cdot z'_i\right)$$
$$+ \sum_{i=1}^{n} \left(c'_i\right)^T \cdot \boldsymbol{Q}_i \cdot z'_i - \left(\sum_{j=1}^{n} \boldsymbol{G}_j \cdot \boldsymbol{Q}_j \cdot r_j\right)^T \cdot \sum_{i=1}^{n} \boldsymbol{G}_i \cdot \boldsymbol{Q}_i \cdot z'_i$$
$$s.t.\ \boldsymbol{T}_i \cdot \boldsymbol{M}'_i \cdot \boldsymbol{Q}_i \cdot z'_i = \boldsymbol{T}_i \cdot b'_i + \boldsymbol{T}_i \cdot \boldsymbol{M}'_i \cdot \boldsymbol{Q}_i \cdot r_i$$
$$\boldsymbol{I}'_{i,sl} \cdot \boldsymbol{Q}_i \cdot z'_i \geq \boldsymbol{I}'_{i,sl} \cdot \boldsymbol{Q}_i \cdot r_i \quad 1 \leq i \leq n,$$

For each participant i ($1 \leq i \leq n$), after calculating and uploading the values of $\boldsymbol{G}_i \cdot \boldsymbol{Q}_i$, $\boldsymbol{G}_i \cdot \boldsymbol{Q}_i \cdot r_i$ and the masked constraints, the cloud server could generate the problem automatically. As all the linear calculation is performed among the local information of participant i, the independence of IM can be preserved.

Appendix B

IM Transformation for Preserving the Problem Scale

After generating $\boldsymbol{T}$, $\boldsymbol{Q}$ and r in the form of equation (18), we can perform IM on equation (1) by transforming it to equation (19). The parameters of equation (18) can be obtained by the following equation:

$$\boldsymbol{F} = \left(\boldsymbol{Q}^\circ\right)^T \cdot \boldsymbol{E} \cdot \boldsymbol{Q}^\circ\ a' = \left(\boldsymbol{Q}^\circ\right)^T \cdot r^\circ - \left(\boldsymbol{Q}^\circ\right)^T \cdot \boldsymbol{E} \cdot \boldsymbol{Q}^\circ \cdot r^\circ$$
$$\boldsymbol{N}^{Eq} = \boldsymbol{T}^{Eq,Eq} \cdot \boldsymbol{M}^{Eq} \cdot \boldsymbol{Q}^\circ$$
$$\boldsymbol{N}^{IE} = \left(\boldsymbol{T}^{IE,Eq} \cdot \boldsymbol{M}^{Eq} + \boldsymbol{T}^{IE,IE} \cdot \boldsymbol{M}^{IE}\right) \cdot \boldsymbol{Q}^\circ$$
$$d^{Eq} = \boldsymbol{T}^{Eq,Eq} \cdot b^{Eq} + \boldsymbol{N}^{Eq} \cdot r^\circ$$
$$d^{IE} = \boldsymbol{T}^{IE,Eq} \cdot b^{Eq} + \boldsymbol{T}^{IE,IE} \cdot b^{IE} + \boldsymbol{N}^{IE} \cdot r^\circ + \boldsymbol{T}^{IE,IE} \cdot \boldsymbol{Q}^{sl} \cdot r^{sl}.$$

Appendix C

In V.C, the Sparsities of the Masked Sub-Matrices for a Region Are Less Than Twice the Original Sparsities

For a sub-power network $\boldsymbol{G}$ with n buses and m branches ($n < m$ without considering the tie lines), define its imaginary part of the node susceptance matrix and node-branch incidence matrix as $\boldsymbol{B}$ and $\boldsymbol{A}$. Here, we generate a tree whose node degrees are in the reverse order relative to those in the original network, and define its node-branch incidence matrix as $\boldsymbol{A}^{Tr}$. In the following passage, we discuss the sparsities of the coefficient matrices $\boldsymbol{B} \cdot |\boldsymbol{A}^{Tr}|$ and $\boldsymbol{A}^T \cdot |\boldsymbol{A}^{Tr}|$ by giving their upper limits using the Chebyshev inequality.

Assume that the branches are represented by $b_1 \cdots b_m$, in which the degree of each bus is represented by $D_1 \cdots D_m$. Denote the sparsities of $\boldsymbol{B}$ and $\boldsymbol{A}$ by $\Omega(\boldsymbol{B})$ and $\Omega(\boldsymbol{A})$. We have

$$\sum_{i=1}^{n} D_i = 2m, \Omega(\boldsymbol{B}) = \frac{2m+n}{n^2}, \Omega(\boldsymbol{A}) = \frac{2}{n}$$

In the generated tree $\boldsymbol{G}^{Tr}$, there should be only n branches, represented by $b_1^{Tr} \cdots b_n^{Tr}$. Define the degree of each node in $\boldsymbol{G}^{Tr}$ as $D_0^{tr} \cdots D_n^{tr}$ (D_0^{tr} represents the degree of the external root), and define the number of the start/end node of b_j^{Tr}, the j^{th} branch of the generated tree, as k_j^{start}/k_j^{end}. According to the definition of the tree, its node-branch incidence matrix A^{tr} should be a non-singular square matrix of $n \times n$ dimensions. In addition, we have:

$$\sum_{i=0}^{n} D_i^{tr} = 2n$$

We begin with $\boldsymbol{B} \cdot |A^{Tr}|$, denoted by Π, whose element in the i^{th} row and j^{th} column is defined as π_{ij}. According to the definitions of $\boldsymbol{B}$ and $\boldsymbol{A}$, for any node i, only when its

adjacent node set S_i (including itself) in the original network is related to b_j^{Tr} can the element π_{ij} be non-zero. Therefore, for any column vector a_j^{Tr} in $|\boldsymbol{A}^{Tr}|$, the quantity of the non-zero elements in $\boldsymbol{B} \cdot a_j^{Tr}$ should be

$$N_j = \begin{cases} D_{k_j^{start}} + D_{k_j^{end}} & b_j^{tr} \notin G \\ D_{k_j^{start}} + D_{k_j^{end}} - 1 & b_j^{tr} \in G \end{cases} \leq D_{k_j^{start}} + D_{k_j^{end}}$$

The quantity of the non-zero elements in Π should meet

$$N(\Pi) = \sum_{j=1}^{n} N_j \leq \sum_{j=1}^{n} D_{k_j^{start}} + D_{k_j^{end}} = \sum_{j=1}^{n} D_j \cdot D_j^{tr}$$

As the node degrees in the generated tree are in the reverse order to those in the original network, according to the Chebyshev inequality, we have:

$$N(\Pi) \leq \sum_{j=1}^{n} D_j \cdot D_j^{tr} \leq \frac{1}{n} \sum_{j=1}^{n} D_j \cdot \sum_{j=1}^{n} D_j^{tr} = 4m$$

Therefore, the sparsity of Π should be

$$\Omega(\Pi) \leq \frac{4m}{n^2} < 2 \cdot \Omega(B)$$

We use a similar method to analyze the sparsity of $\Phi = \boldsymbol{A}^T \cdot |\boldsymbol{A}^{Tr}|$, denoted by $\Omega(\Phi)$, whose element in the i^{th} row and j^{th} column is defined as φ_{ij}.

The dimensions of Φ should be $m \times n$. According to the definitions of $\boldsymbol{A}^T$ and $|\boldsymbol{A}^{Tr}|$, φ_{ij} can be non-zero when and only when $b_i \cap b_j^{Tr} \neq 0$ and $b_i \neq b_j^{Tr}$. Therefore, for any column vector in $|\boldsymbol{A}^{Tr}|$, a_j^{Tr}, the quantity of the non-zero elements in $\boldsymbol{A}^T \cdot a_j^{Tr}$ is the same as that in $\boldsymbol{B} \cdot a_j^{Tr}$, based on which we can similarly estimate $\Omega(\Phi)$:

$$\Omega(\Phi) \leq \frac{4m}{mn} = \frac{4}{n} = 2 \cdot \Omega(\boldsymbol{A})$$

The result of the case study on an IEEE 118-bus system in Fig. 6 verifies this conclusion. Notably, $\Omega(\Pi)$ and $\Omega(\Phi)$ further decrease as the system scale increases, which is acceptable for the optimal computation and information storage.

REFERENCES

[1] X. Shi, Y. Li, Y. Cao, and Y. Tan, "Cyber-physical electrical energy systems: Challenges and issues," *CSEE J. Power Energy Syst.*, vol. 1, no. 2, pp. 36–42, Jun. 2015.

[2] L. Feng, J. Zhang, G. Li, and B. Zhang, "Cost reduction of a hybrid energy storage system considering correlation between wind and PV power," *Prot. Control Mod. Power Syst.*, vol. 1, no. 1, pp. 1–9, 2016.

[3] S. Rusitschka, K. Eger, and C. Gerdes, "Smart grid data cloud?: A model for utilizing cloud computing in the smart grid domain," in *Proc. 1st IEEE Int. Conf. Smart Grid Commun.*, 2010, pp. 483–488.

[4] B. Bitzer and T. Kleesuwan, "Cloud-based smart grid monitoring and controlling system," in *Proc. Power Eng. Conf. (UPEC)*, Stoke-on-Trent, U.K., 2015, pp. 1–5.

[5] S. Bera, S. Misra, and J. J. P. C. Rodrigues, "Cloud computing applications for smart grid?: A survey," *IEEE Trans. Parallel Distrib. Syst.*, vol. 26, no. 5, pp. 1477–1494, May 2015.

[6] H. Kim *et al.*, "Cloud-based demand response for smart grid: Architecture and distributed algorithms," in *Proc. IEEE Int. Conf. Smart Grid Commun. (SmartGridComm)*, Brussels, Belgium, 2011, pp. 398–403.

[7] B. Bitzer and E. S. Gebretsadik, "Cloud computing framework for smart grid applications," in *Proc. Power Eng. Conf. (UPEC)*, Dublin, Ireland, 2013, pp. 1–5.

[8] Y. Simmhan, A. G. Kumbhare, B. Cao, and V. Prasanna, "An analysis of security and privacy issues in smart grid software architectures on clouds," in *Proc. IEEE 4th Int. Conf. Cloud Comput. (CLOUD)*, Washington, DC, USA, 2011, pp. 582–589.

[9] S. Baktir, "Privacy preserving smart grid management in the cloud," in *Proc. Int. Conf. IT Converg.*, Security, Beijing, China, 2014, pp. 1–4.

[10] A. Jacobsson, M. Boldt, and B. Carlsson, "On the risk exposure of smart home automation systems," in *Proc. Int. Conf. Future Internet Things Cloud (FiCloud)*, Barcelona, Spain, 2014, pp. 183–190.

[11] N. Saxena and B. J. Choi, "Integrated distributed authentication protocol for smart grid communications," *IEEE Syst. J.*, to be published.

[12] J. Yao and P. Venkitasubramaniam, "The privacy analysis of battery control mechanisms in demand response: Revealing state approach and rate distortion bounds," in *Proc. IEEE 53rd Annu. Conf. Decis. Control (CDC)*, vol. 6. Los Angeles, CA, USA, 2014, pp. 1377–1382.

[13] D.-H. Choi and L. Xie, "Ramp-induced data attacks on look-ahead dispatch in real-time power markets," *IEEE Trans. Smart Grid*, vol. 4, no. 3, pp. 1235–1243, Sep. 2013.

[14] J. Kim and L. Tong, "On topology attack of a smart grid: Undetectable attacks and countermeasures," *IEEE J. Sel. Areas Commun.*, vol. 31, no. 7, pp. 1294–1305, Jul. 2013.

[15] D. Wu, F. Ma, M. Javadi, and J. N. Jiang, "Fast screening severe cyber attacks via transient energy-based impact analysis," *CSEE J. Power Energy Syst.*, vol. 2, no. 3, pp. 28–34, Sep. 2016.

[16] J. Chen *et al.*, "Impact analysis of false data injection attacks on power system static security assessment," *J. Mod. Power Syst. Clean Energy*, vol. 4, no. 3, pp. 496–505, 2016.

[17] A. R. Borden, D. K. Molzahn, P. Ramanathan, and B. C. Lesieutre, "Confidentiality-preserving optimal power flow for cloud computing," in *Proc. 50th Annu. Allerton Conf. Commun. Control Comput.*, Monticello, IL, USA, 2012, pp. 1300–1307.

[18] A. R. Borden, D. K. Molzahn, B. C. Lesieutre, and P. Ramanathan, "Power system structure and confidentiality preserving transformation of optimal power flow problem," in *Proc. 51st Annu. Allerton Conf. Commun. Control Comput.*, Monticello, IL, USA, 2013, pp. 1021–1028.

[19] J. Dreier and F. Kerschbaum, "Practical privacy-preserving multiparty linear programming based on problem transformation," in *Proc. IEEE 3rd Int. Conf. IEEE Soc. Comput. Privacy Security Risk Trust (PASSAT) (SocialCom)*, Boston, MA, USA, 2011, pp. 916–924.

[20] D. Wu, B. C. Lesieutre, and P. Ramanathan, "Feasibility of power system structure preserving linear transformations for the AC optimal power flow problem," in *Proc. Allerton Conf. Commun. Control. Comput.*, Monticello, IL, USA, 2014, pp. 715–722.

[21] W. Zheng, W. Wu, B. Zhang, H. Sun, and Y. Liu, "A fully distributed reactive power optimization and control method for active distribution networks," *IEEE Trans. Smart Grid*, vol. 7, no. 2, pp. 1021–1033, Mar. 2016.

[22] Q. Guo, S. Xin, H. Sun, Z. Li, and B. Zhang, "Rapid-charging navigation of electric vehicles based on real-time power systems and traffic data," *IEEE Trans. Smart Grid*, vol. 5, no. 4, pp. 1969–1979, Jul. 2014.

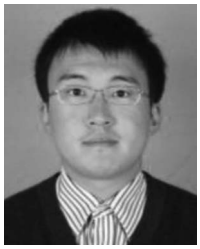

Shujun Xin (S'13) received the bachelor's degree from the Department of Electrical Engineering, Tsinghua University in 2012, where he is currently pursuing the Ph.D. degree. His research interests include cyber-physical system and V2G technology.

Qinglai Guo (SM'14) received the B.S. degree from the Department of Electrical Engineering, Tsinghua University, Beijing, China, in 2000, and the Ph.D. degree from Tsinghua University in 2005 where he is currently an Associate Professor. His research interests include energy management system, voltage stability and control, cyber-physical system, renewable energy integration, and electric vehicles.

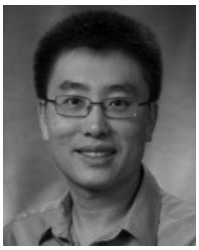

Jianhui Wang (M'07–SM'12) received the Ph.D. degree in electrical engineering from the Illinois Institute of Technology, Chicago, IL, USA, in 2007.

He is currently an Associate Professor with the Department of Electrical Engineering, Southern Methodist University, Dallas, TX, USA. He also holds a joint appointment as the Section Lead for Advanced Power Grid Modeling with the Energy Systems Division, Argonne National Laboratory, Argonne, IL, USA. He has held visiting positions in Europe, Australia, and Hong Kong including a VELUX Visiting Professorship with the Technical University of Denmark.

Dr. Wang was a recipient of the IEEE Power and Energy Society (PES) Power System Operation Committee Prize Paper Award in 2015. He is the Secretary of the IEEE PES Power System Operations, Planning and Economics Committee. He is an Associate Editor of the *Journal of Energy Engineering* and an Editorial Board Member of *Applied Energy*. He is the Editor-in-Chief of the IEEE TRANSACTIONS ON SMART GRID. He is an IEEE PES Distinguished Lecturer.

Chen Chen (M'13) received the B.S. and M.S. degrees from Xi'an Jiaotong University, Xi'an, China, in 2006 and 2009, respectively, and the Ph.D. degree in electrical engineering from Lehigh University, Bethlehem, PA, USA, in 2013. From 2013 to 2015, he was a Post-Doctoral Researcher with the Energy Systems Division, Argonne National Laboratory, Argonne, IL, USA, where he is currently a Computational Engineer. His primary research is in optimization, communications and signal processing for smart electric power systems, cyber-physical system modeling for smart grids, and power system resilience.

Hongbin Sun (SM'12) received the double B.S. degrees in 1992 and the Ph.D. degree from the Department of Electrical Engineering in 1997 from Tsinghua University. He is currently a Changjiang Chair Professor of the Education Ministry of China, a Full Professor of electrical engineering with Tsinghua University, and an Assistant Director of the State Key Laboratory of Power Systems, China. From 2007 to 2008, he was a Visiting Professor with the School of EECS, Washington State University, Pullman.

In the last 15 years, he has developed a commercial system-wide automatic voltage control systems which has been applied to over 20 large-scale power grids in China. He published over 200 academic papers. He holds over 20 patents in China. He was a recipient of the China National Technology Innovation Award for his contribution on successful development and applications of New Generation of EMS for Power Systems in 2008, the National Distinguished Teacher Award in China for his contribution on power engineering education in 2009, and the National Science Fund for Distinguished Young Scholars of China for his contribution on power system operation and control in 2010. He is an IET Fellow and a member of IEEE PES CAMS Cascading Failure Task Force and CIGRE C2.13 Task Force on Voltage/Var support in System Operations.

Boming Zhang (SM'95–F'10) received the Ph.D. degree in electrical engineering from Tsinghua University, Beijing, China, in 1985. Since 1985, he has been with the Electrical Engineering Department, Tsinghua University, for teaching and research and promoted to a Professor in 1993. His interest is in power system analysis and control, especially in the EMS advanced applications in the Electric Power Control Center (EPCC). He has published over 300 academic papers and implemented over 60 EMS/DTS systems in China. He is currently a Steering Member of CIGRE China State Committee and of the International Workshop of EPCC.